# Reaction processes in a $He_2^+(C\,^2\Pi_u \rightarrow A\,^2\Sigma_g^+)$ flash lamp

Peter Collin Hill and Peter Robert Herman
*Department of Electrical and Computer Engineering, University of Toronto, Toronto, Ontario, Canada M5S 1A4*
(Received 31 July 1992)

The reaction processes in a $He_2^+(C\,^2\Pi_u \rightarrow A\,^2\Sigma_g^+)$ flash lamp (600-Torr, 10-cm-long, pulsed capillary discharge) are analyzed to estimate the spontaneous emission rate and a device gain. The observed dominance of $He_2^+(C\,^2\Pi_u \rightarrow A\,^2\Sigma_g^+)$ radiation over all other radiative transitions, together with predicted rates for these radiative transitions, are used to characterize the plasma. New reactions are proposed between $He(2\,^3P)$ and the ground-state molecular ions that produce $He_2^+(C\,^2\Pi_u)$ by rapid two-body momentum exchanges and explain the absence of $He(2\,^3P)$ and ground-state molecular ions in the discharge. A first approximation that all ion-electron recombinations result in $He_2^+(C\,^2\Pi_u)$ provides a conservative gain estimate of 0.4% per meter for this device. $He_2^+(C\,^2\Pi_u \rightarrow B\,^2\Sigma_g^+)$ absorption is identified as a key loss process that will limit the tuning range of a potential laser. An investigation of excimer laser discharges reveals the presence of the $He_2^+(C\,^2\Pi_u)$ molecule at pressures of 0.1–10 atm.

PACS number(s): 33.80.−b, 82.40.Ra, 42.72.Bj, 52.80.Mg

## I. INTRODUCTION

The recently identified $He_2^+(C\,^2\Pi_u)$ state [1,2] is of general interest because its three electrons are all in binding orbitals. This is reflected in the shape of its potential curve, which helps to explain the unusual properties of $He_2^+(C\,^2\Pi_u)$: (1) the shortest known molecular bond length of $r_e = 0.69$ Å (theoretical value from Ref. [3]) and $r_e = 0.56$ Å (semiempirical value from Ref. [1]), which supersede that of $He_2^{2+}$, $r_e = 0.7251$ Å [4], and $H_2$, $r_e = 0.74$ Å; (2) bright spontaneous emission over a large spectral range [1] of 1500–8000 Å, which has led to the recent proposal [1] for a tunable laser in the range of 2000–8000 Å; and (3) a high formation temperature [1] of > 3000 K. In a discharge, conditions of high pressure and high temperature can be so favorable for the production of $He_2^+(C\,^2\Pi_u)$ that neutral $He_2^*$, with its competing $A\,^1\Sigma_u^+ \rightarrow X\,^1\Sigma_g^+$ radiation at 600–1000 Å, is almost entirely absent. To date, e-beam experiments have investigated only low-temperature ( < 1000 K) He plasma and have therefore failed to identify this potential line of laser development. The $He_2^+(C\,^2\Pi_u)$ light source is also of fundamental importance as an efficient broadband source of ultraviolet light [5].

Lack of knowledge about the lifetime and populations of $He_2^+(C\,^2\Pi_u)$ makes difficult an estimate of device gain, and has thereby discouraged experimental investigation of this potential laser. Although the molecule can be produced in a wider range of conditions than most excimers, it is well understood that because its wide spectral range is broader than most excimers (spectral width ~10 Å), the relative gain per molecule is diminished by ~500 times. However, helium flash lamps are intense and efficient sources [5], and may produce sufficient densities of $He_2^+(C\,^2\Pi_u)$ for laser operation. The absolute photon flux from a $He_2^+(C\,^2\Pi_u \rightarrow A\,^2\Sigma_g^+)$ lamp has not been measured, albeit helium, because of its fundamental nature and use as a buffer gas, has been extensively characterized. Drawing on this information, this paper aims to theoretically predict the $He_2^+(C\,^2\Pi_u)$ production rate and photon flux inside existing discharge sources to determine whether sufficient gain is available for a $He_2^+(C\,^2\Pi_u \rightarrow A\,^2\Sigma_g^+)$ laser, and hence whether further experimental investigation is merited. Perhaps of equal importance, an understanding of the gas kinetics will be developed that gives insight into the formation of helium dimer ions in general.

The $He_2^+(C\,^2\Pi_u \rightarrow A\,^2\Sigma_g^+)$ continuum has now been identified in an increasing variety of devices: dc capillary discharges [6], dc arcs [1], ac discharges [1], and flash lamps [1]. In addition, we have produced the spontaneous continuum in a high-pump-power excimer-laser discharge filled with pure helium. The dimer ion continuum was observed in the visible and recorded in the vacuum-ultraviolet (VUV) spectral region (1000–2000 Å) by a VUV intensified photodiode array (Princeton Electronics model CMSA ST-130 TE/CCD). The emissions were observed from 100 Torr to 10 atm, greatly extending the upper-limit pressure of 800 Torr previously observed [5] for this molecular ion. However, the complex discharge kinetics have precluded a definitive interpretation of the time-resolved spectra, favoring the flash lamp [600 Torr, 10 $cm^2$, inside diameter (i.d.) 0.7 cm] built by Huffman, Tanaka, and Larrabee [5] as the most worthy of analysis for evaluation of device gain. Detailed spectra in the 300–4500-Å spectral region, which include He* and $He_2^*$ features, provide important information on populations and ion densities. Below, a gain calculation for the flash lamp is based directly on an estimated light production rate, namely, the product of the radiative lifetime and the population of the upper state, circumventing direct determination of these elusive upper-state parameters.

## II. $He_2^+(C\,^2\Pi_u)$ FORMATION MECHANISMS

In a pulsed electric helium discharge [7] (1 atm, $N_e = 10^{15}$ $cm^{-3}$, $T_e = 2000$ K), there is no evidence of $He_2^+(C\,^2\Pi_u \rightarrow A\,^2\Sigma_g^+)$ radiation, while neutral molecular $He_2(A\,^1\Sigma_u^+ \rightarrow X\,^1\Sigma_g^+)$ radiation dominates the emis-

 

sion spectrum. Stevefelt, Pouvesle, and Bouchoule [7] estimated a 60% $He_2(A\,^1\Sigma_u^+ \rightarrow X\,^1\Sigma_g^+)$ radiation yield, which arises solely from $He_2^+(X\,^2\Sigma_u^+)$ recombination. The lack of ion-dimer radiation may be explained by the dc-arc experiment by Simon and Rodgers [8]. Comparison of the region of their arc producing $He_2^+(C\,^2\Pi_u \rightarrow A\,^2\Sigma_g^+)$ emission ([8], Fig. 7) with their temperature profile ([8], Fig. 12) shows that a higher temperature of $T > 3200$ K is required for the ion-dimer transition, necessary to overcome a 1-eV barrier [1] in the $C$-state potential.

In the Huffman flash lamp, a 0.06-$\mu$F capacitor was connected directly across the electrodes and then charged until spontaneous breakdown at a voltage of $\sim 10$ kV. Considering that Huffman's flash lamp must produce a similar high temperature, as well as a higher electron density [1] of $N_e = 3.3^{+6.7}_{-2.1} \times 10^{16}$ cm$^{-3}$, it is not surprising that the high-temperature emissions by the flash lamp and dc arc are dramatically altered compared to that recorded by Stevefelt, Pouvesle, and Bouchoule [7]. The Huffman flash lamp produces almost no neutral molecular radiation [5], while over 75% of all emission arises solely from the ion-molecule (compare [5], Fig. 2 with [1], Fig. 2). In this paper, an approximation is made that 100% $He_2^+(C\,^2\Pi_u \rightarrow A\,^2\Sigma_g^+)$ radiation yield arises from all recombinations, justified by the development of an understanding of the molecular ion formation mechanisms, an assessment of the impact of these mechanisms on the plasma kinetics, and a consideration of loss mechanisms.

An analysis of the $He_2^+(C\,^2\Pi_u \rightarrow A\,^2\Sigma_g^+)$ spectrum and relevant potential curves [1] leads one to consider the following $He_2^+(C\,^2\Pi_u)$ formation reactions:

$$He^+ + He(2\,^3P) + X \Longrightarrow He_2^+(C\,^2\Pi_u) + X\ , \qquad (X = \text{He, e, etc.})\ , \quad (1a)$$

$$He_n^+ + He(2\,^3P) \Longrightarrow He_2^+(C\,^2\Pi_u) + (n-1)He\ , \qquad (n = 2,3,4)\ , \quad (1b)$$

or

$$He_2^* + He^+ \Longrightarrow He_2^+(C\,^2\Pi_u) + He\ . \quad (1c)$$

The upper state decays radiatively according to

$$He_2^+(C\,^2\Pi_u) \Longrightarrow He_2^+(A\,^2\Sigma_g^+) + \gamma(1500\text{–}8000\ \text{Å})\ , \quad (2)$$

or

$$He_2^+(C\,^2\Pi_u) + \gamma \Longrightarrow He_2^+(A\,^2\Sigma_g^+) + 2\gamma\ , \quad (3)$$

followed by the dissociation reaction,

$$He_2^+(A\,^2\Sigma_g^+) \Longrightarrow He^+ + He(1\,^1S)\ . \quad (4)$$

The reactions in Eq. (1) have a formation energy barrier [1] of approximately 1 eV. At temperatures near 3000 K, quasibound $He_2^+(C\,^2\Pi_u)$ states enhance molecule formation, while these elevated temperatures diminish the barrierless $He_2^+(X\,^2\Sigma_u^+)$ formation. Electron collisions in Eq. (1a) merit more consideration than usual in this plasma because (1) electrons are lighter, traveling some 85 times faster than He, and undergo correspondingly more collisions; and (2) electrons are charged, resulting in Coulomb scattering with ions, which, at a temperature of 3200 K, have a collision cross section [9] $10^4$ times greater than that with neutral He. These two factors produce an overall electron-ion collision frequency that is 200 times larger than the neutral-ion frequency at $N_e = 10^{16}$ cm$^{-3}$. Notwithstanding this, Eq. (1a) requires a momentum-conserving collision, which must occur during the brief time the ion and $He(2\,^3P)$ are within a bond length of each other.

Enhancement of the ion-molecule formation rate by Coulombic collisions is not restricted to $He_2^+(C\,^2\Pi_u)$ but will also apply more generally to $He_n^+$. Formation of $He_2^+(C\,^2\Pi_u)$ through the ion-molecule channel of Eq. (1b) can proceed comparatively rapidly, as momentum is conserved by the dissociation of neutral helium in this two-body collision. A complementary reaction involves a helium atom bonding with $He(2\,^3P)$ to form $He_2^*$, which in turn reacts [Eq. (1c)] with the ion to produce $He_2^+(C\,^2\Pi_u)$.

The possibility that Eq. (1b) or Eq. (1c) may dominate the commonly proposed reaction of Eq. (1a) is a general concept that may be profitably applied to other plasmas. The observed high yield [10] of quartet dimer ions [dissociation products: $He^+ + He(2\,^3S)$] in weak low-pressure discharges is currently an enigma. The quartet dimer ions have a lifetime of many $\mu$s and an identified drift velocity faster than $He_2^+(X\,^2\Sigma_u^+)$. The extremely low concentrations of reactants preclude three-body formation analogous to Eq. (1a), instead favoring formation through a momentum exchange analogous to Eq. (1b), between $He_2^+(X\,^2\Sigma_u^+)$ and $He(2\,^3S)$. It is further submitted that vibrationally excited $He_2^+(X\,^2\Sigma_u^+)$ is required for quartet formation. In this way, the reduced yield of quartet dimer ions observed at higher pressure can be understood by vibrational relaxation of $He_2^+(X\,^2\Sigma_u^+)$ by collisions.

Equations (2) and (3) are, respectively, the spontaneous and the stimulated radiative channels for the decay of the upper state, which is followed by the dissociation of the lower state according to Eq. (4). If the He ion is considered as a temperature-activated catalyst that extracts a photon from $He(2\,^3P)$, then Eqs. (1)–(4) contract, yielding the following formula for spontaneous emission:

$$He(2\,^3P) \xrightarrow[He^+,\ T > 3200\ K]{} He(1\,^1S) + \gamma(1500\text{–}8000\ \text{Å})\ . \quad (5)$$

The lower state, $He_2^+(A\,^2\Sigma_g^+)$, is unbound, thereby automatically producing population inversion for $He_2^+(C\,^2\Pi_u)$ and satisfying one criterion for a laser transition. Clearly, at a sufficiently high ion density and in the right temperature conditions, the $He_2^+(C\,^2\Pi_u)$ reaction path given by Eq. (1) will proceed vigorously. The question is: what density is sufficient for laser action? Ion densities as high as $10^{18}$ cm$^{-3}$ have been reported [8] in a dc arc (250 A, 5000 Torr), but high temperatures may cause the $He_2^+(C\,^2\Pi_u)$ molecule to dissociate. In the cooler pulsed flash lamp (600 Torr), the ion concentration [1] is $3.3 \times 10^{16}$ cm$^{-3}$ and the $He_2^+(C\,^2\Pi_u)$ continuum dominates all other line sources. In this pressure region, a number of approximations become valid and the

TABLE I. Helium flash lamp reactions.

| Eq. no. | Process | Reaction (branching ratio %) | Rate | Magnitude in flash lamp[a] $r$ = rate ($cm^{-3}\,s^{-1}$) $t$ = lifetime (ns) | Ref. |
|---|---|---|---|---|---|
| (6) | Radiation trapping | $He^* \Longrightarrow He(1\,^1S)+\gamma_{resonance}$ | (rate) = (natural rate)/$g$,[b] $g = 1.12/\sqrt{\pi k_0 R}$ | $t \gg 0.5$ | [11–14] |
| (7) | Ionization continuum absorption | $He(2\,^3S)+\gamma \Longrightarrow He^+ + e$ | $5.2\times10^{-20}$ $cm^2$ absorption edge at 2580 Å | not observed | [15,16] |
| (8) | Collisional recombination<br>Atomic | $He_2^+ 2e \Longrightarrow$ { $He(2\,^3S)+e$ 19%; $He(2\,^1S)+e$ 6%; $He(2\,^1P)+e$ 19%; $He(2\,^3P)+e$ 56% } | $3.55\times10^{14}T_e^{-11}$ | $r = 1\times10^{24}$<br>$t = 10$ | [18–21] |
| | Molecular | $He_2^+(X\,^2\Sigma_u^+)+2e \Longrightarrow He_2(A\,^1\Sigma_u^+)+e$<br>$\Longrightarrow He_2(X\,^1\Sigma_u^+)+e+\gamma$ >60% | ~atomic rate | minor contribution | [9] |
| (9) | Trimer formation and<br>Rydberg dissociative recombination | $He_2^+(X\,^2\Sigma_u^+)+He+X \Longrightarrow He_3^+ + X$<br>$He_3^+ + e \Longrightarrow$ { $He(2\,^1P)+2He$ 25%; $He(2\,^3P)+2He$ 75% } | $1.0\times10^{-26}\times\left[\frac{435}{T_e}\right]^2$ | $t = 18$ | [17,23] |
| (10) | Weak spin exchange[c] | $He(2\,^1S)+e \Longrightarrow He(2\,^3S)+e'$ | $3.5\times10^{-7}$ | $t = 0.3$ | [25] |
| (11) | Electron impact electronic transitions[c] | $He(2\,^3P)+e \Longrightarrow$ $He(2\,^3S)+e'$ | $8.4\times10^{-9}T_e^{1/3}$ | $t = 0.8$ | [26] |
| | | $He(2\,^1S)+e'$ | $3.1\times10^{-8}/(1+T_e/16360)$ | $t = 2.7$ | |
| | | $He(2\,^1P)+e'$ | $1.8\times10^{-7}/(1+T_e/8180)$ | $t = 0.4$ | |
| (12) | Superelastic collisions | $e+He(2\,^3S)$, $e+He(2\,^3P) \Longrightarrow He(1\,^1S)+e'$ | $4.1\times10^{-9}/(1+T_e/17460)$ | $t = 20$ | [26] |
| | | | $2.1\times10^{-10}$ | $t = 476$ | |
| | | $e+He_2^* \Longrightarrow 2He+e'$ | $4.0\times10^{-9}$ | $t = 20$ | [17] |
| (13) | Coulombic collisions | $e+He^+ \Longrightarrow He^+ + e'$ | $3.64T_e^{-3/2}$ $\times \ln(1.24\times10^7/T_e^{3/2}N_e^{-1/2})$ | $t = 0.0005$ | [27] |
| (14) | Electron-electron impact thermalization | $e+e' \Longrightarrow e''+e'''$ | $6.6T_e^{3/2}$ | $t = 0.003$ | [28] |
| (15) | Auto-ionization-assisted vibrational relaxation | $He_2^+(v=m)+e \Longrightarrow He_2^*(v=n)$<br>$\Longrightarrow He_2^+(v=m-1)+e'$, | $\approx \frac{5.4\times10^{-17}\lambda}{T_e^{3/2}}$ | $t = 0.056$ | [29] |
| | | $He_2^+(v=m-1)+e \Longrightarrow He_2^*(v=n-1)$<br>$\Longrightarrow He_2^+(v=m-2)+e'$<br>$\vdots$ | $\times \ln\left[\frac{5.2\times10^{22}}{\lambda}\left[\frac{T_e^3}{N_e}\right]^{0.915}\right]$ | | |
| | | $\Longrightarrow He_2^+(v=0)+e''$ | $(\lambda = 10^{15})$ | | |
| | Example: associative ionization | $He(3\,^3D)+He \Longrightarrow He_2^* \Longrightarrow He_2^+ + e$ | $6\times10^{-10}$ | $t = 0.06$ | [30] |
| (16) | Dimer formation | $He(2\,^3S)$, $He(2\,^3P)$, $He(2\,^1P)$ $+2He \Longrightarrow He_2^* + He$ | $9.2\times10^{-34}$ | $t = 10\,000$ | [17,32] |
| | | | $1.6\times10^{-32}$ | $t = 69$ | [31] |
| | | | $1.8\times10^{-31}$ | $t = 6$ | [31] |
| | | $He^+ + 2He \Longrightarrow He_2^+ + He$ | $1.1\times10^{-31}$ $\times(T_{gas}/300)^{-0.38}$ | $t = 20$ | [33] |
| | | $He^+ + He + e \Longrightarrow He_2^+ + e$ | —— | | |

[a]For conditions: $N_e = 10^{16}$ $cm^{-3}$, [He] = $3\times10^{19}$ $cm^{-3}$, $T_e = 3200$ K, $T_{gas} = 3200$ K.
[b]$R$ = radius of excited volume, $k_0$ = maximum absorbance of pressure-broadened transition.
[c]Deexcitation rate; excitation rate found by detailed balance.

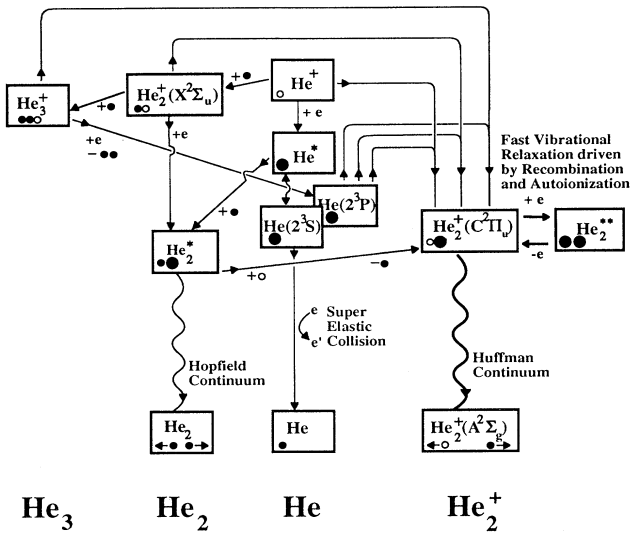


FIG. 1. Schematic of important reaction pathways producing the Huffman and Hopfield continua. Atoms are represented by: He($1\,^1S$) ●, He* ●, and $He^+$ ○.

calculation of the gain becomes feasible.

It is evident from Eq. (1) that the population of He($2\,^3P$) is important in determining the production rate of $He_2^+(C\,^2\Pi_u)$ and ultimately a gain value. For the Huffman flash lamp operated with a spark gap in the Hopfield mode, spectrograph plates [Ref. [5], Fig. 4(a)] clearly show the presence of the forbidden He($2\,^3P \rightarrow 1\,^1S$) line, which can be used to determine the He($2\,^3P$) population. With the spark gap, the flash lamp is sufficiently cool for $He_2^*$ formation, but not for $He_2^+(C\,^2\Pi_u)$. In higher-pressure and -temperature He discharges, where the capacitor is connected directly across the electrodes and charged until breakdown, the 1500–8000-Å continuum [Ref. [5], Figs. 4(b)–4(d)] of $He_2^+(C\,^2\Pi_u \rightarrow A\,^2\Sigma_g^+)$ is produced intensely, while the He($2\,^3P$) line is no longer evident. This indicates a very low He($2\,^3P$) equilibrium population and is consistent with a very high conversion rate, as per Eq. (1), of He($2\,^3P$) into $He_2^+(C\,^2\Pi_u)$, which is faster than the He($2\,^3P$) formation rate. Conversely, if Eq. (1) was the rate-limiting step in the production of the molecule, the strength of the continuum radiation produced would require an appreciable population of He($2\,^3P$), and evidence of its own line radiation. The experimental evidence indicates that the production rate of the molecular ion is the production rate of He($2\,^3P$), prompting a wider investigation of plasma kinetics to determine the formation rate of He($2\,^3P$).

## III. PLASMA KINETICS

The high electron densities of the flash lamp lead electron collisions to overtake radiation as the major transition mechanism between excited states. Unlike radiative processes favoring transitions among energetically separate states, electron collision cross sections are large between states of small energy separation. For this reason, excited states of helium, He*, rapidly form into He($2\,^3P$). Table I summarizes important reactions that occur under high-pressure, high-electron-density conditions. Rates and lifetimes are calculated for the plasma conditions specific to the Huffman flash lamp. The most significant reactions, together with Eq. (1), are shown schematically in Fig. 1. Each of these reactions will now be discussed in detail to develop an overall picture of the plasma kinetics.

Radiation trapping [Table I, Eq. (6)], the absorption and reemission of radiation by the abundant ground-state helium, inhibits radiative decay of resonant states. This extends their apparent lifetime by a factor $g$, derived by Holstein [11,12] and van Trigt [13,14]. The calculated lifetime refers to radiation escaping through the side of the capillary; the spectra that are taken from an axial view will shown greatly diminished resonance radiation. Radiation trapping, together with the existence of numerous metastable states that are dipole and/or spin forbidden to radiate, make atomic helium a poor radiator in these discharge conditions. Molecule formation that forms new symmetries permitting radiation and quenching are the major loss mechanisms for He*.

Ionization continuum absorption [Table I, Eq. (7)] by He* will be a loss mechanism in a $He_2^+(C\,^2\Pi_u \rightarrow A\,^2\Sigma_g^+)$ laser. This absorption will become resonant near the ionization thresholds of the various excited states, creating a sawtooth absorption structure. The highly populated $2\,^3S$ state should display an absorption edge near 2600 Å. However, since a population of $10^{15}$ $cm^{-3}$ is calculated to absorb about 3% of the flash lamp radiation on this resonance, and there is no evidence of this effect in the spectrum of Ref. [5], Fig. 2, it is submitted that this absorption is not a major loss mechanism for the laser.

Fortuitously, collisional $He^+$ recombination [Table I, Eq. (8)] has a branching ratio [17] of 56% directly to the He($2\,^3P$) state. Recombination rates increase [18–21] with the third power of the electron density, but at $T_e > 3000$ K, change from a $T_e^{-5}$ to a $T_e^{-11}$ dependence. The same mechanism and rate apply for the recombination of the ground-state dimer ion $He_2^+(X\,^2\Sigma_u^+)$. Molecular ion recombination, however, would necessarily result in neutral molecular radiation, namely, the Hopfield continuum—$He_2(A\,^1\Sigma_u^+ \rightarrow X\,^1\Sigma_g^+)$, from 600 to 1000 Å. The $He_2(A\,^1\Sigma_u^+)$ state ($D_e = 2.55$ eV [22]) has no dissociative channels and is thus expected to withstand high temperatures. It is estimated [7] that the branching ratio for the production of the Hopfield continuum on recombination of $He_2^+(X\,^2\Sigma_u^+)$ is 60%. This large value can be understood when one considers the enhanced number of bound states that are produced by avoided crossings of electronic states. The radiation of neutral molecular bands is very weak in the flash lamp, and becomes weaker as the $He_2^+(C\,^2\Pi_u \rightarrow A\,^2\Sigma_g^+)$ continuum strengthens with increasing pressure, raising the question: where is the $He_2^+(X\,^2\Sigma_u^+)$ population?

Rydberg dissociative recombination [23] [Table I, Eq. (9)] occurs when high pressures convert the $He_2^+(X\,^2\Sigma_u^+)$ dimers to trimers before they can recombine. Unlike dimers, trimers have a dissociative channel that can dispose

of excess momentum in recombination. In a longitudinal flash lamp, the onset of trimer formation restricts the production of neutral dimer radiation by recombination to pressures of $<100$ Torr. Rydberg dissociative recombination is strongly favored by a $T_e^{-2}$ rate dependence, rather than a $T_e^{-11}$ dependence, for collisional radiative recombination, and can proceed faster than collisional recombination at sufficiently high pressures and electron temperatures. However, as the flash lamp rates for these two processes shown in Table I are of similar size, trimer formation can not solely explain the weakness of neutral-dimer radiation. The trimer, with $D_e = 0.17$ eV [24], will be in thermal equilibrium with the population of $He_2^+(X\,^2\Sigma_u^+)$ at flash lamp temperatures of 3200 K. If the trimer forms and then reacts with $He(2\,^3P)$ according to Eq. (1b), the ion-dimer continuum will be in direct competition with the neutral-dimer continuum, helping to explain the weakness of the latter. The trimer is seen to have alternative reaction paths that either destroy [Eq. (1b)] or create [Eq. (9)] $He(2\,^3P)$.

Weak spin-exchange reactions [Table I, Eq. (10)] were discovered by Phelps [25], who observed a rapid decay of the $He(2\,^1S)$ population in afterglows. Other electron-impact electron transitions [Table I, Eq. (11)] have subsequently been measured [26]. Their speed rapidly establishes thermal equilibrium. For a temperature of 3000 K, the $He(2\,^3P)$ state should have a population similar in size to that of the $He(2\,^1P)$ and $He(2\,^1S)$ states, while $\sim 96\%$ of the $n=2$ population will reside in the $He(2\,^3S)$ state. The observed weakness of the $He(2\,^3P)$ line, noted above, implies a more rapid conversion of $He(2\,^3P)$ to the molecule via Eq. (1) than the 0.4-ns time for $He(2\,^3P)$ formation by electron impacts.

Superelastic collisions [26] [Table I, Eq. (12)] are a major He* loss mechanism in these plasma conditions, proceeding more quickly than radiative channels. Instead of escaping as radiation, energy stored in He* heats the electron energy distribution, creating a nonthermal electron distribution of energies that plateau up to a threshold corresponding to the metastable excitation energy. The afterglow energy distribution function (EDF) will reflect the ratio of heating collisions (with He*) and cooling collisions [27] [mostly from Coulombic collisions with ions; Table I, Eq. (13)]. Electrons can exchange and average momentum [Table I, Eq. (14)], rapidly steering the EDF towards a Boltzmann distribution. The formation of the molecular ion [Eq. (1)] and subsequent radiation by Eqs. (2) and (3) diminishes the relative He* population, thereby reducing the EDF heating, and leading to increased recombination, according to Eq. (8). The $He_2^+(C\,^2\Pi_u)$ formation and radiation cycle [Eqs. (1)–(4)] diverts energy from the electrons into both the heavy-body temperature and radiation.

In most discharges, the relative intensity of the $n>2$ He I lines are diminished with respect to resonant $He(2\,^1P \rightarrow 1\,^1S$; 584 Å) lines because of lower Boltzmann populations and lower dipole transition moments. At high pressures, further reductions arise from the possibility of associative ionization, which has a cross section many orders of magnitude higher than for simple association. This large value occurs because, for $n>2$, the $He_2^*$ state potential overlaps the $He_2^+(X\,^2\Sigma_u)$ potential, permitting autoionization assisted vibrational relaxation [29] [Table I, Eq. (15)]. This process greatly enhances the formation rate of the molecule by removing the $He_2^*$ at the vibrational energy at which it is formed more quickly than through the usual collisional channels. This model successfully predicts the measured [30] associative ionization rate of $He(3\,^3D)$, the example shown in Table I, Eq. (15). A similar mechanism is also available to $He_2^+(C\,^2\Pi_u)$. In this case, the neutral state would be formed from dissociation products of $He(2\,^3P)$ and another high-lying ($n>40$) Rydberg state [29], forming part of a Rydberg series of molecular curves that approaches the $He_2^+(C\,^2\Pi_u)$ potential. $He_2^+(C\,^2\Pi_u)$ formation rates will be enhanced by this channel of vibrational energy loss shown in Fig. 1.

Finally, dimer formation by three-body collisions will be examined [Table I, Eq. (16)]. $He_2^*$ formation, particularly from $He(2\,^1P)$, can be extremely rapid [31]. As with He*, electron impacts will promptly mix the electronic states of $He_2^*$. Combination of He and $He(2\,^1P)$, followed by radiative decay, produces $He_2(A\,^1\Sigma_u^+)$, which has a lifetime [2] of 0.55 nsec for radiative decay to $He_2(X\,^1\Sigma_g^+)$. As this latter radiation is only weakly observed in the flash lamp, and other neutral molecular transitions are negligible, we are left to conclude that $He_2^*$ is either not produced or very quickly forms $He_2^+(C\,^2\Pi_u)$, according to Eq. (1c). This conclusion is consistent with the observed weakness of the $He(2\,^1P \rightarrow 1\,^1S)$ 584-Å line compared to higher members of the series seen in the flash lamp spectra (Ref. [5], Fig. 3). The analysis of $He_2^*$ formation offers a second potential reaction mechanism tying the competition observed between the Hopfield and Huffman continua, and places a minimum value, namely, $<6$ nsec, on the $He_2^+(C\,^2\Pi_u)$ formation rate, which must be faster than the highest dimer formation rate [Table I, Eq. (16)].

The reaction rates surveyed here show that electron collisions dominate radiative processes within He* and $He_2^*$. However, their precise contribution to the ion-molecule formation rate is yet to be determined. Trimer ion formation was found to be important for its impact on recombination, as well as the formation and the destruction of $He(2\,^3P)$. But the precise details of the mechanism by which $He_2^+(C\,^2\Pi_u)$ supplants $He_2^*$ radiation, as evidenced by the spectra, are still to be uncovered. The arguments consistently support a high $He_2^+(C\,^2\Pi_u)$ yield following all recombination processes, but have so far ignored competing processes such as He*-electron deexcitation.

## IV. $He_2^+(C\,^2\Pi_u)$ FORMATION RATE

The populations of $He_2^+(C\,^2\Pi_u)$ and He* will be in thermal equilibrium if rates of electron-impact transitions amongst the He* states, $He_2^+(C\,^2\Pi_u)$ formation rates [Eq. (1)], and vibrational relaxation rates are rapid compared with upper-state decay rates. The $v=0$ level of $He_2^+(C\,^2\Pi_u)$ is calculated [1] to be 19.8 eV above the $He_2^+(X\,^2\Sigma_u)$ dissociation energy, coinciding with the energy of the $He(2\,^3S)$ state, and thereby sharing the same

equilibrium population per energy level. However, due to rotation, $He_2^+(C\,^2\Pi_u)$ has over 50 more energy levels and will have a correspondingly larger population. This population weighting ensures that superelastic $He(2\,^3S)$ collisions that occur every 20 ns in the flash lamp [Table I, Eq. (12)] are subordinate to $He_2^+(C\,^2\Pi_u)$ losses discussed in Sec. V.

The spectral evidence and above arguments indicate that the rate-limiting step for $He_2^+(C\,^2\Pi_u \rightarrow A\,^2\Sigma_g^+)$ radiation is not the formation of $He_2^+(C\,^2\Pi_u)$, nor the formation of $He(2\,^3P)$, but is fundamentally limited by He* formation rates. Equation (5) may be reexpressed to approximate the spontaneous emission rate for this flash lamp as

$$\mathrm{He}^* \xrightarrow[\mathrm{He}^+,\ T>3200\ \mathrm{K}]{} \mathrm{He}(1\,^1S)+\gamma(1500\text{–}8000\ \text{Å})\ . \quad (17)$$

That is to say: all He* eventually forms the molecule and the rate for Eq. (17) may be approximated by the recombination rate. Simply by determination of the He* formation rate, an approximate upper bound can be placed on the spontaneous emission rate and thence the gain, for coarse evaluation of the feasibility of a laser device. Further consideration of the fraction of He* lost through other channels, as well as nonradiative $He_2^+(C\,^2\Pi_u)$ decay processes in the plasma discharge, are warranted for full assessment of the laser potential.

## V. $He_2^+(C\,^2\Pi_u)$ LOSS MECHANISMS

Several potential loss mechanisms are evaluated for their ability to arrest laser action on the $He_2^+(C\,^2\Pi_u \rightarrow A\,^2\Sigma_g^+)$ transition. As with all lasers, loss mechanisms directly associated with the upper-state $He_2^+(C\,^2\Pi_u)$ will be diminished by competition with an enhanced stimulated emission rate through the use of an optical cavity or a seed laser. These types of losses, while effecting the small signal gain, have limited impact on the operating efficiency of a laser. Also worthy to note is the reduced significance of $He_2^+(C\,^2\Pi_u)$ loss mechanisms producing He* products, as these products were seen to rapidly reform $He_2^+(C\,^2\Pi_u)$.

One example of a loss mechanism in direct competition with stimulated emission is

$$He_2^+(C\,^2\Pi_u)+e \rightleftharpoons He^+ + He^* + e\ . \quad (18)$$

The cross section for collisions between charged species is noted to be high. However, since Eq. (18) is also a formation process of He*, which in turn produces $He_2^+(C\,^2\Pi_u)$ by Eq. (1), this loss mechanism can be considered to have an overall null effect in the gain calculation. However, if ground-state He arises as a reaction product in Eq. (18), a significant loss results that merits further estimation by *ab initio* calculation in order to assess the restricted plasma conditions in which the laser can operate.

A related loss mechanism is electron-impact ionization,

$$He_2^+(C\,^2\Pi_u)+e \rightleftharpoons He_2^{2+}+e+e \rightleftharpoons He^+ + He^+ + e + e\ . \quad (19)$$

The threshold energy for this reaction is 6.5 eV, 2 eV above the energy of the products at infinity [34]. This process is energetically less accessible than its atomic equivalent, electron-impact ionization of He*, that opposes the He-ion recombination reaction given by Eq. (8) in Table I. The rate given with Eq. (8) is empirically based on equilibrium processes that implicitly include loss reactions like He* electron-impact ionization. Then, losses like Eq. (19) are automatically accommodated by use of the Eq. (8) rate in the laser gain calculation of Sec. VI.

The quartet dimer ion is known to produce excited singlet species on recombination [2], which under spin conservation, further implies the production of an excited triplet state as well. This supports a hypothesis proposing the formation of two He* on recombination of $He_2^+(C\,^2\Pi_u)$:

$$He_2^+(C\,^2\Pi_u)+e+e \rightleftharpoons He^* + He^* + e\ . \quad (20)$$

The molecular ion recombination rate can be approximated by the $He^+$ recombination rate in Eq. (8) of Table I. However, much like Eq. (18), this reaction should not be considered a loss mechanism for $He_2^+(C\,^2\Pi_u)$ because of the strong equilibrium favoring its reformation from He*.

The strong He II line emissions observed in the flash lamp result from a high $He^{2+}$ population and constitute a loss of energy. $He^{2+}$ can be formed by electron impact of $He^+$ at threshold energies above 54.4 eV, prompting investigation of possible reactions producing such energetic electrons. Studies [35,36] of the electron EDF resulting from superelastic collisions show two plateaus. The first terminates at the atomic metastable-state energy. The second, much diminished, plateau results from electrons in this first plateau undergoing a second superelastic collision. At best, double superelastic collisions provide only 49 eV, falling short of the requisite threshold. The possible formation of two ground-state helium atoms from $He_2^+(C\,^2\Pi_u)$ collisional recombination given by Eq. (20), taking into account the ($13\pm3$ eV) potential energy of the nuclei [37], could result in electrons of approximately $32\pm3$ eV energy. In the case of two collisions with $He_2^+(C\,^2\Pi_u)$, this would lead to maximum energies of 74 eV, sufficient for the production of $He^{2+}$. Another possibility for $He^{2+}$ production is the direct two-body reaction,

$$He_2^+(C\,^2\Pi_u)+He_2^+(C\,^2\Pi_u) \rightleftharpoons He^{2+}+3He\ , \quad (21)$$

as each $He_2^+(C\,^2\Pi_u)$ has up to 45 eV of energy available. One of the colliding dimers could also be a Rydberg state, which would eliminate the Coulombic repulsive barrier. The proposed reaction, while explaining the second EDF plateau, constitutes a new loss mechanism for the proposed laser. Although theoretical calculations of potential surfaces are required for a definitive rate, this reaction can be compared with the equivalent neutral metastable-metastable reaction [17] having a typical rate of $1.5\times10^{-9}\ \mathrm{cm}^{-6}\,\mathrm{s}^{-1}$. The maximum extent of this loss process in the flash lamp is estimated to be $<3\%$ by noting the strength of the He II radiation relative to the total light output of the Huffman continuum.

As with all excimers, radiative excitation of the upper laser states by absorption of its own stimulated radiation can critically hamper laser performance by rendering the gas absorbing. The $He_2^+(B\,^2\Sigma_g^+)$ is the only excited state that has the appropriate symmetry and radial-wave-function overlap (Ref. [1], Fig. 2) for absorption:

$$He_2^+(C\,^2\Pi_u)+\gamma \Longrightarrow He_2^+(B\,^2\Sigma_g^+) . \tag{22}$$

Since $He_2^+(B\,^2\Sigma_g^+)$ is formed from the same valence and Rydberg diabatic states as $He_2^+(A\,^2\Sigma_g^+)$, they will share similar transition moments from the $C$ state. However, the wave-function overlap will be substantially larger for $He_2^+(B\,^2\Sigma_g^+)$. Examination of the potential curves [1] for the respective states reveals that absorption from $He_2^+(C\,^2\Pi_u)$ to the free and quasibound states of $He_2^+(B\,^2\Sigma_g^+)$ may eliminate laser action for the short-wavelength end of the spontaneous spectrum. Further losses can arise by electron-impact conversion of the $C$ state to the $B$ state. Photoabsorption studies and more accurate *ab initio* calculation of the $B$-state potential are warranted to determine the full extent of this effect. Once formed, $He_2^+(B\,^2\Sigma_g^+)$ will quickly dissociate or decay to $He_2^+(X\,^2\Sigma_u)$ by spontaneous or possibly by stimulated radiation in the region of 560 Å. In the flash lamp of Huffman, strong bands exist in this region that are yet to be assigned. For the gain calculation, a sufficiently long wavelength will be assumed to preclude $He_2^+(B\,^2\Sigma_g^+)$ absorption.

## VI. GAIN

The plasma in a flash lamp goes through two stages: excitation and recombination. During excitation, the upward pressure of electron collisions maintains [9] a greater $He(2\,^3P)$ population than $He(2\,^3S)$. The populations depend on the electric fields and gas densities and are difficult to characterize. The He* population arising from recombination depends only on the electron density and temperature and is thus easier to characterize. The He* formation rate and the laser gain calculation are based on a recombining plasma.

By careful characterization of a flash lamp (66 cm long, 200 Torr, $N_e=7\times10^{14}$ cm$^{-3}$, $T_e=3200$ K, $T_{\text{heavy body}}=1200$ K), Carman [9] showed that the collisional recombination rate of Eq. (8) self-consistently models the plasma dynamics, yielding a recombination rate of $3.4\times10^{20}$ cm$^{-3}$ s$^{-1}$. This value constitutes a conservative minimum rate for the Huffman lamp conditions (10 cm, 600 Torr, $N_e>1.2\times10^{16}$ cm$^{-3}$), where at least a 5000-fold increase in recombination is expected due to the greater ion density, and possible enhancement afforded by the more swift trimer recombination has been ignored. However, unexplored temperature effects and new reaction channels may moderate this increased rate, and the more conservative value will be used below.

The approximation in Eq. (17), that each recombination results in the proposed laser transition, gives a spontaneous emission rate of $r=3.4\times10^{20}$ photons cm$^{-3}$ s$^{-1}$. This value is modest in comparison with the measured [38] $He_2(A\,^1\Sigma_u \rightarrow X\,^1\Sigma_g^+)$ radiative rate of $1.1\times10^{21}$ cm$^{-3}$ s$^{-1}$ for a 1-atm transverse flash lamp.

The usual equation for stimulated emission per unit length of the device, $g$, is

$$g=N\sigma=N\lambda^4/(8\pi c\tau\Delta\lambda) , \tag{23}$$

where $N$ is the density of $He_2^+(C\,^2\Pi_u)$, $\lambda$ is the wavelength, $c$ is the speed of light, $\tau$ is the upper-state lifetime, and $\Delta\lambda$ is the spontaneous emission bandwidth, estimated to be 1500 Å (Ref. [1], Fig. 2). Given a spontaneous emission rate of $r=N/\tau$, the gain becomes

$$g=r\lambda^4/(8\pi c\Delta\lambda) . \tag{24}$$

Introducing a diminution of 10 to account for the reduced strength at the peak cross section of stimulated emission [1] ($\lambda=6050$ Å), together with the above recombination rate for $r$, yields

$$g=r\times1.2\times10^{-25}=4\times10^{-5}\ \text{cm}^{-1} . \tag{25}$$

This conservative estimate yields a small 0.4% gain over a 1-m gain length. However, considering that this result is based on a device not yet optimized for pressure, current, and capillary size, suggests that a laser, for which the mirror loss is less than the gain, could be successfully demonstrated. Based on the breadth of the spontaneous spectrum, laser action could be broadly tunable from ~3000 Å to the infrared. This, together with the fact that the laser employs a single inexpensive noble gas, suggests not only that the laser may be feasible but that it may have practical applications.

## VII. CONCLUSION

Since the discovery of the $He_2^+(C\,^2\Pi_u)$ state, the shape of the potential curves and high-brightness flash lamp emissions have illuminated the possibility of a very broadband laser. The above investigation of the kinetics shows that this brightness and the feasibility of this laser rests on the very high ion density supporting a high recombination rate to the excited states of helium. In turn, high temperatures favor rapid production of $He_2^+(C\,^2\Pi_u)$ from these excited states, most likely through a two-body momentum exchange. A gain calculation showed that the $He_2^+(C\,^2\Pi_u)$ production rate is sufficient to overcome the low gain per molecule that results from the broadband width of the electronic state emission. It is hoped that the present gain result will stimulate further experimental work in the development of a $He_2^+$ laser, and the measurement of its photon flux and electron and excited state densities, in order to shed further light on the reaction processes in a $He_2^+(C\,^2\Pi_u \rightarrow A\,^2\Sigma_g^+)$ flash lamp.

## ACKNOWLEDGMENT

The authors would like to thank Sebastian Jaimungal for his assistance in recording the $He_2^+(C\,^2\Pi_u \rightarrow A\,^2\Sigma_g^+)$ emission in an excimer laser cavity.

[1] P. Hill, Phys. Rev. A **43**, 2546 (1991).
[2] P. Hill, Phys. Rev. A **40**, 5006 (1989).
[3] J. Ackermann and H. Hogreve, Chem. Phys. **157**, 75 (1991).
[4] P. Gill and L. Radom, Chem. Phys. Lett. **132**, 16 (1986).
[5] R. Huffman, Y. Tanaka, and J. Larrabee, J. Opt. Soc. Am. **52**, 851 (1962).
[6] J. Mentel (private communication).
[7] J. Stevefelt, J. Pouvesle, and A. Bouchoule, J. Chem. Phys. **76**, 4006 (1982).
[8] D. Simon and K. Rodgers, J. Appl. Phys. **37**, 2255 (1966).
[9] R. Carman, IEEE J. Quantum Electron. **26**, 1558 (1990).
[10] J. Madson, H. Oskam, and L. Chanin, Phys. Rev. Lett. **15**, 1018 (1965).
[11] T. Holstein, Phys. Rev. **72**, 1212 (1947).
[12] T. Holstein, Phys. Rev. **83**, 1159 (1951).
[13] C. van Trigt, Phys. Rev. **181**, 97 (1969).
[14] C. van Trigt, Phys. Rev. A **1**, 1298 (1970).
[15] V. Jacobs, Phys. Rev. A **9**, 1938 (1974).
[16] K. McCann and M. Flannery, Appl. Phys. Lett. **31**, 599 (1977).
[17] R. Deloche, P. Monochchicourt, M. Cheret, and F. Lambert, Phys. Rev. A **13**, 1140 (1976).
[18] L. Biberman, V. Vorobev, and T. Yakubov, Usp. Fiz. Nauk **107**, 353 (1972) [Phys. Usp. **15**, 375 (1973)].
[19] E. Hinnov and J. Hirschberg, Phys. Rev. **125**, 795 (1962).
[20] D. Bates, K. Bell, and A. Kingston, Proc. Phys. Soc. London **91**, 228 (1967).
[21] R. Motely and A. Kucks, in *Proceedings of the 5th International Conference on Ionization Phenomena in Gases,* edited by H. Maecker (North-Holland, Amsterdam, 1961).
[22] A. Laslett Smith, J. Chem. Phys. **49**, 4817 (1968).
[23] D. Bates, J. Phys. B **17**, 2363 (1984).
[24] K. Balasubramamian, M. Liao, and S. Lin, Chem. Phys. Lett. **142**, 349 (1987).
[25] A. Phelps, Phys. Rev. **99**, 1307 (1955).
[26] R. Berrington, P. Burke, L. Freitas, and A. Kingston, J. Phys. B **18**, 4135 (1985).
[27] M. Mitchener and C. Kruger, Jr., *Partially Ionized Gas* (Wiley, New York, 1973).
[28] D. Book, *NRL Plasma Formulary* (NRL, Washington, DC, 1987).
[29] J. Stevefelt, Phys. Rev. A **8**, 2507 (1973).
[30] M. Teter, F. Niles, and W. Robertson, J. Chem. Phys. **44**, 3018 (1966).
[31] F. Emmert, H. Angermann, R. Dux, and H. Langoff, J. Phys. D **21**, 677 (1988).
[32] G. Myers and A. Cunningham, J. Chem. Phys. **67**, 247 (1977).
[33] J. Russell, J. Chem. Phys. **84**, 4344 (1986).
[34] H. Yagisawa, H. Sato, and T. Watanabe, Phys. Rev. **16**, 1352 (1977).
[35] C. Gorse, J. Bretange, and M. Capitelli, Phys. Lett. A **126**, 277 (1988).
[36] J. Mizeraczky, J. Phys. D **17**, 1647 (1984).
[37] P. Foreman, P. Roi, and K. Coffin, J. Chem. Phys. **61**, 1658 (1974).
[38] M. Gand, A. Bouchoule, and J. Stevefelt, Appl. Phys. Lett. **35**, 50 (1979).